RESEARCH ARTICLE | *Neurogastroenterology and Motility*

Histamine causes influx via T-type voltage-gated calcium channels in an enterochromaffin tumor cell line: potential therapeutic target in adverse food reactions

Beatrix Pfanzagl,[1] Victor F. Zevallos,[3] Detlef Schuppan,[3] Roswitha Pfragner,[4] and Erika Jensen-Jarolim[1,2]

[1]*Institute of Pathophysiology and Allergy Research, Center for Pathophysiology, Infectiology, and Immunology, Medical University of Vienna, Vienna, Austria;* [2]*The Interuniversity Messerli Research Institute, University of Veterinary Medicine Vienna, Medical University of Vienna, University Vienna, Vienna, Austria;* [3]*Division of Molecular and Translational Medicine, Department of Medicine I, Johannes Gutenberg University, Mainz, Germany; and* [4]*Otto Loewi Research Center for Vascular Biology, Immunology, and Inflammation, Medical University of Graz, Graz, Austria*

Pfanzagl B, Zevallos VF, Schuppan D, Pfragner R, Jensen-Jarolim E. Histamine causes influx via T-type voltage-gated calcium channels in an enterochromaffin tumor cell line: potential therapeutic target in adverse food reactions. *Am J Physiol Gastrointest Liver Physiol* 316: G291–G303, 2019. First published December 12, 2018; doi:10.1152/ajpgi.00261.2018.—The P-STS human ileal neuroendocrine tumor cells, as a model for gut enterochromaffin cells, are strongly and synergistically activated by histamine plus acetylcholine (ACh), presumably via histamine 4 receptors, and weakly activated by histamine alone. Sensing these signals, enterochromaffin cells could participate in intestinal intolerance or allergic reactions to food constituents associated with elevated histamine levels. In this study we aimed to analyze the underlying molecular mechanisms. Inhibition by mepyramine and mibefradil indicated that histamine alone caused a rise in intracellular calcium concentration ($[Ca^{2+}]_i$) via histamine 1 receptors involving T-type voltage-gated calcium channels (VGCCs). Sensitivity to histamine was enhanced by pretreatment with the inflammatory cytokine tumor necrosis factor-α (TNF-α). In accordance with the relief it offers some inflammatory bowel disease patients, otilonium bromide, a gut-impermeable inhibitor of T-type (and L-type) VGCCs and muscarinic ACh receptors, efficiently inhibited the $[Ca^{2+}]_i$ responses induced by histamine plus ACh or by histamine alone in P-STS cells. It will take clinical studies to show whether otilonium bromide has promise for the treatment of adverse food reactions. The cells did not react to the nutrient constituents glutamate, capsaicin, cinnamaldehyde, or amylase-trypsin inhibitors and the transient receptor potential channel vanilloid 4 agonist GSK-1016790A. The bacterial product butyrate evoked a rise in $[Ca^{2+}]_i$ only when added together with ACh. Lipopolysaccharide had no effect on $[Ca^{2+}]_i$ despite the presence of Toll-like receptor 4 protein. Our results indicate that inflammatory conditions with elevated levels of TNF-α might enhance histamine-induced serotonin release from intestinal neuroendocrine cells.

NEW & NOTEWORTHY We show that histamine synergistically enhances the intracellular calcium response to the physiological agonist acetylcholine in human ileal enterochromaffin tumor cells. This synergistic activation and cell activation by histamine alone largely depend on T-type voltage-gated calcium channels and are inhibited by the antispasmodic otilonium bromide. The cells showed no response to wheat amylase-trypsin inhibitors, suggesting that enterochromaffin cells are not directly involved in nongluten wheat sensitivity.

amylase trypsin inhibitors; calcium channels; enterochromaffin; histamine; otilonium bromide

INTRODUCTION

At present, the triggers of adverse food reactions in individual patients are not entirely predictable. Innate mechanisms and neuronal factors may amplify the reactions, especially with preexisting inflammatory conditions. While most research so far has been dedicated to mast cells, eosinophils, and macrophages, we propose here that enterochromaffin (EC) cells might participate in and amplify adverse food symptoms or impact the threshold levels for clinical symptoms.

EC cells are dispersed throughout the intestinal mucosa and release serotonin (5-hydroxytryptamine) to the serosal side upon stimulation by nutrients or other chemical mediators, acidic pH, or mechanical distortion (6, 25). Their apical microvilli project in the gut lumen. They are found in close contact to nerve endings of submucosal neurons of the enteric reflex pathways, which are largely cholinergic (26, 36). Cholinergic agonists like acetylcholine (ACh) induce a rise in intracellular calcium ($[Ca^{2+}]_i$) that triggers exocytosis of serotonin-containing vesicles to the basolateral side (46). ACh (26) and serotonin (21, 29, 62) enhance gut secretion and motility, and high levels of serotonin can cause diarrhea (60). A role of serotonin in the pathology of inflammatory bowel disease, diarrhea-predominant irritable bowel syndrome (IBS), and celiac disease is also discussed (19, 20, 30).

The P-STS cell line (45, 48), isolated from a poorly differentiated neuroendocrine tumor of the terminal ileum, grows with a stable genotype (48) and was established as a reliable EC cell line by showing stable expression of the neuroendocrine vesicle components and tryptophanhydroxylase-1, the rate-limiting enzyme for synthesis of serotonin expressed specifically in enteroendocrine cells (44). The neuroendocrine identity of P-STS cells was confirmed by Hofving et al. (27), as was the neuroendocrine origin of

Address for reprint requests and other correspondence: B. Pfanzagl, Inst. of Pathophysiology and Allergy Research, Medical University of Vienna, Waehringer Guertel 18-20, A-1090, Vienna, Austria (e-mail: beatrix.pfanzagl @meduniwien.ac.at).

 G291

the GOT1 cell line derived from a liver metastasis of an ileal serotonin-producing tumor. To date, these two cell lines are the only established models for human intestinal serotonin-producing (EC) cells (24). The higher serotonin content of GOT1 cells (27) suggests that they might be suitable for studies of serotonin secretion, while the P-STS cell line contains only a small amount of serotonin (44). Whether GOT1 cells like P-STS cells respond to a physiologically appropriate stimulus like ACh (44) apparently has not been investigated.

P-STS cells react to histamine with a strong increase in $[Ca^{2+}]_i$ when it is added simultaneously with ACh that exceeds the $[Ca^{2+}]_i$ increase evoked by ACh alone (44). There was also a similar reaction in the presence of ACh with the histamine 4 receptor (H_4R) ligand 4-methylhistamine (4-mHA), suggesting an involvement of H_4R. We now established that the $[Ca^{2+}]_i$ response to ACh plus histamine is more than additive. There was also a weak response to histamine 1 receptor (H_1R) that had not been noticed previously. We investigated the role of external calcium and of L-, N-, P-, R-, and T-type voltage-gated calcium channels (VGCC) in the responses of P-STS cells to ACh and histamine. Voltage-dependent calcium currents in primary ileal neuroendocrine tumor cells cultivated for a few days have been attributed mainly to L-type VGCC (22). Influx of calcium can also be mediated by transient receptor potential (TRP) channels. Some of them can be activated by food constituents like cinnamaldehyde [transient receptor potential channel ankyrin 1 (TRPA1)], capsaicin [transient receptor potential channel vanilloid 1 (TRPV1)], or piperine (TRPA1 and TRPV1). TRPA1, TRPV1, and transient receptor potential channel vanilloid 4 (TRPV4) have been implicated in nociception (5) and thus might be involved in IBS. Accordingly, we also investigated the reaction of P-STS cells to agonists of these channels.

Our search for other potential activators of serotonin release present in greater amounts in the human diet included the flavor enhancer glutamate and the short-chain fatty acid butyrate produced by bacterial degradation of fiber (57). The $[Ca^{2+}]_i$ response of P-STS cells to wheat amylase-trypsin inhibitors (ATI) was also investigated. ATI are nongluten proteins highly resistant to intestinal proteolysis that are taken up with wheat and related cereals (67). They activate the innate intestinal immune responses via Toll-like receptor 4 (TLR4) on monocytes/macrophages or dendritic cells (28), inducing the release of inflammatory cytokines. As established for bacterial lipopolysaccharide (LPS), these effects of ATI require the presence of CD14 as part of the TLR4-MD2-CD14 complex.

METHODS

Cell culture. P-STS midgut neuroendocrine tumor cells [semi-adherent, originally isolated from a World Health Organization III neuroendocrine tumor of the terminal ileum (48)] were grown in a 1:1 mixture of medium-199 and Ham's F-12 nutrient mixture supplemented with 10% heat-inactivated fetal calf serum, 100 U/ml penicillin G, and 100 μg/ml streptomycin at 37°C in a humidified atmosphere containing 5% CO_2. HEK 293 human embryonic kidney cells and THP-1 monocytes were grown in DMEM and RPMI 1640 medium, respectively, containing the same supplements. THP-1 cells were differentiated for 2 days with 200

nM phorbol 12-myristate,13-acetate (PMA) before immunofluorescence staining or treatment with LPS. All cell lines were tested for mycoplasma contamination by staining with Hoechst dye 33342.

Antibodies and reagents. Mouse anti-human TLR4 antibody (clone 76B357.1) was from Novus Biologicals (Littleton, CO); rabbit anti-human phospho-NF-κB p65(Ser536) (clone 93H1) was from Cell Signaling Technology (Cambridge, UK); mouse anti-human RelA/NF-κB p65 (clone 532301) and recombinant human tumor necrosis factor-α (TNF-α) were from R&D Systems (Minneapolis, MN); rabbit anti-human TRPV4 (directed against an epitope in the middle region) and the corresponding blocking peptide were from Aviva Systems Biology (San Diego, CA); Alexa Fluor 647-labeled mouse anti-human CD14 was from Biolegend (San Diego, CA); goat Alexa Fluor 488-labeled secondary fluorescent antibodies and fluo 4-AM were from Life Technologies (Carlsbad, CA); mouse anti-human H_1R (G-11) and the corresponding blocking peptide as well as anti-mouse IgG-horseradish peroxidase were from Santa Cruz Biotechnology (Dallas, TX); ω-agatoxin IVA, 4-methylhistamine dihydrochloride, mepyramine maleate, mibefradil dihydrochloride, and rantidine hydrochloride were from Tocris (Bristol UK); ω-conotoxin GVIA was from Smartox Biotechnology (Saint-Egrève, France); SNX-482 was from Peptanova (Sandhausen, Germany); otilonium bromide was from Seleckchem (Munich, Germany); L-epinephrine, capsaicin, piperine, *trans*-cinnamaldehyde (99%), A-23187 Ca^{2+} ionophore, nifedipine, GSK-1016790A, PMA, LPS from *Escherichia coli* 055:B5, bovine serum albumin (>98%), ACh chloride, histamine dihydrochloride, monosodium L-glutamic acid, and sodium butyrate were from Sigma Aldrich (St. Louis, MO).

Isolation of wheat ATI. Wheat ATI was isolated as described elsewhere (67). Briefly, wheat kernels were ground to flour, sieved (250 μm), defatted with methanol/diethylether, dried, and extracted with 50 mM ammonium bicarbonate/0.3 M sodium chloride (pH 7.8) at 4°C. The extract was fractionated with ammonium sulfate. The fraction precipitating between 1.8 and 4 M ammonium sulfate was redissolved, extensively dialyzed against 10 mM ammonium bicarbonate/0.3 M sodium chloride (pH 7.8), cleared by centrifugation, filtered (0.22 μm), and freeze-dried, resulting in a preparation with an ATI content of ~60% of total protein known to contain mainly the isoforms CM3, 0.19, and 0.28, as determined by mass spectrometry (67). Biological activity and endotoxin content below 0.1 ng/mg were ascertained as described elsewhere (67). Before use, the ATI preparation was resuspended in water at a concentration of 30 mg dry wt/ml.

Immunofluorescence microscopy and $[Ca^{2+}]_i$ imaging. For immunofluorescence microscopy, cells were grown on cover slips and analyzed as described previously (44). Briefly, cells were fixed with 4% paraformaldehyde in phosphate-buffered saline (PBS) and permeabilized for 5 min with 0.2% vol/vol Triton X-100 in PBS. Blocking and incubation with antibodies took place in 5% fetal calf serum in PBS at room temperature. Nuclei were stained with Hoechst dye 33342. Where indicated, antibodies were preincubated for 2 h at room temperature with or without a fivefold (weight/weight) amount of blocking peptide corresponding to their epitope before addition to the fixed and permeabilized cells.

$[Ca^{2+}]_i$ imaging with fluo 4-AM, quantification with Image J, and statistical analysis of $[Ca^{2+}]_i$ responses from ranked data with the unpaired two-tailed *t*-test assuming unequal variances were done as described previously (44). Briefly, the cells were grown in 24-well plates to very low density and stained 45 min at room temperature with fluo 4-AM in serum-free medium. The medium was exchanged for 200 μl pure medium, and, after 25 min of incubation at room temperature, photographs were taken before and after careful addition of potential agonists in 200 μl pure medium. The $[Ca^{2+}]_i$ response of fluo 4-AM-stained P-STS cells to addition of the indicated substances was determined as fluorescence enhancement 10 s after the start of

substance addition in relation to baseline fluorescence, if not indicated otherwise. The number of experiments conducted (n) is given in the legends for Figs 1–10.

For evaluation of the effect of external calcium, cells were washed two times with HEPES-buffered saline, pH 7.4, without Ca^{2+} after incubation with fluo 4-AM and then incubated for 25 min in the same buffer with or without 1 mM Ca^{2+} before agonist addition.

RNA isolation, reverse transcription, and polymerase chain reaction. RNA from 50% confluent P-STS cells was isolated, purified, and quantified with TRIzol (Thermo Fisher Scientific, Waltham, MA) following the manufacturer's instructions. In a total volume of 20 μl, cDNA was synthesized from 0.7 μg RNA using the iScriptcDNA Synthesis Kit (Bio-Rad) as described by the manufacturer and kept at −20°C until use. Polymerase chain reaction (PCR) amplifications were performed with 0.1 μl cDNA. *Thermus aquaticus* Taq DNA polymerase and deoxynucleotides were from Sigma Aldrich. The amplification process was started with incubation at 95°C for 5 min. After 35–42 cycles (see below) elongation was completed for 7 min at 72°C. The following primer pairs (ordered from Thermo Fisher Scientific) and PCR conditions were used successfully: human H_4R forward 5′-CCG TTT GGG TGC TGG CCT TCT TAG-3′ and reverse 5′-GAT CAC GCT TCC ACA GGC TCC AAT-3′ [product size 204 bp (55)] with 1.5 mM $MgCl_2$ and 40 cycles (30 s at 95°C, 30 s at 60°C, 1 min at 72°C);

human TRPV4 forward 5′-GAG AAC ACC AAG TTT GTC ACC A-3′ and reverse 5′-TGA ATC ATG ATG CTG TAG GTC C-3′ [product size 632 and 812 bp (32)] with 2.5 mM $MgCl_2$ and 42 cycles (30 s at 95°C, 1 min at 60°C, 1 min at 72°C); human H_1R PrimerBank (53) primer pair ID 149158708c2 (forward 5′-CTG AGC ACT ATC TGC TTG GTC-3′ and reverse 5′-AGG ATG TTC ATA GGC ATG ACG A-3′, product size 158 bp) with 1.5 mM $MgCl_2$ and 35 cycles (30 s at 95°C, 1 min at 54°C, 1 min at 72°C); human free fatty acid receptor 2 (FFAR2) PrimerBank primer pair ID 227430361c2 (forward 5′-TGC TAC GAG AAC TTC ACC GAT-3′ and reverse 5′-GGA GAG CAT GAT CCA CAC AAA AC-3′, product size 135 bp, conditions as for human H_4R); human free fatty acid receptor 3 (FFAR3) PrimerBank primer pair ID 209862766c2 (forward 5′-GCG TGG AGG ATC TAC GTG AC-3′ and reverse 5′-TGT GAG TGT TCA CTG GTC TTT C-3′, product size 233 bp) with 1.5 mM $MgCl_2$ and eight cycles with annealing at 60°C (30 s at 95°C, 30 s at 60°C, 1 min at 72°C) plus 32 cycles at 54°C (30 s at 95°C, 1 min at 54°C, 1 min at 72°C); human TLR4 PrimerBank primer pair ID 373432602c1 (forward 5′-AGA CCT GTC CCT GAA CCC TAT-3′ and reverse 5′-CGATGGACTT-CTAAACCAGCCA-3′, expected product 147 bp, conditions as for human H_4R). PCR products and Thermo Scientific GeneRuler DNA Ladder Mix were separated on 1% agarose and stained with ethidium bromide.
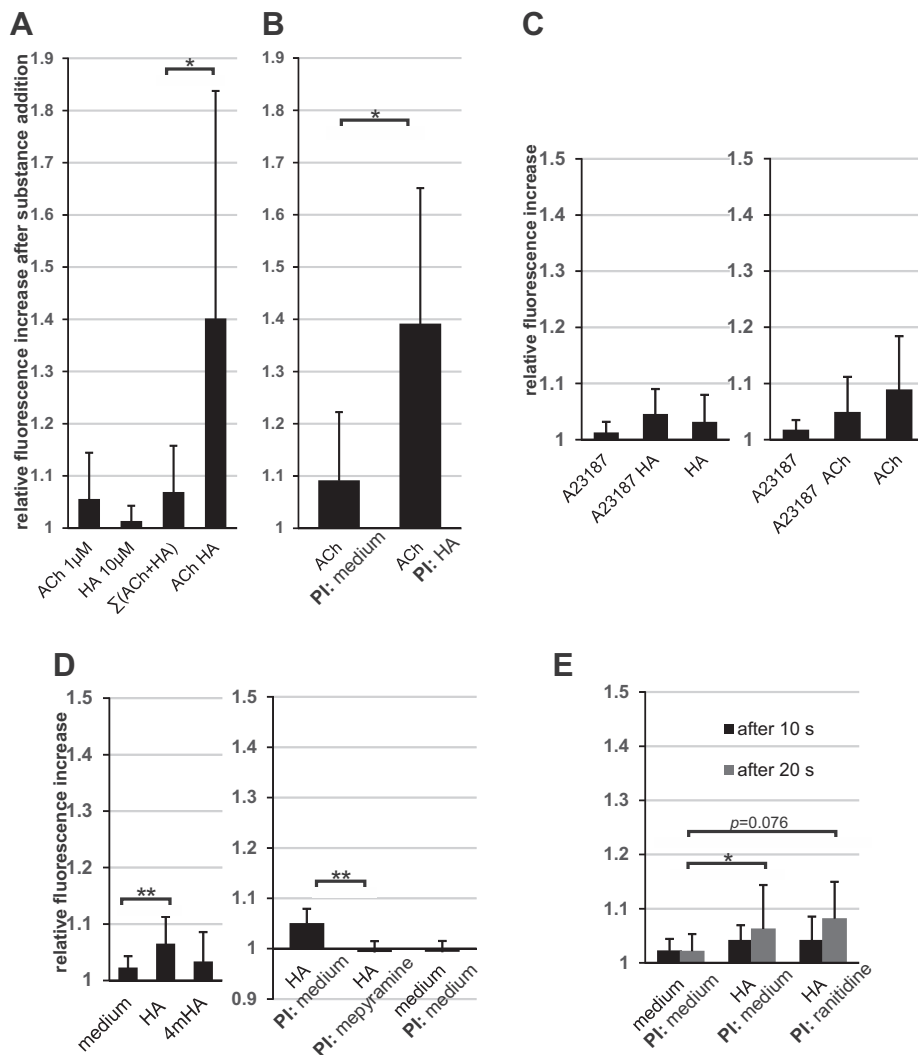

Fig. 1. The intracellular calcium concentration ($[Ca^{2+}]_i$) response of fluo 4-AM-stained P-STS cells to histamine and other substances. For preincubation (PI), the indicated substances were added to the cells 10 min before agonist addition. HA, histamine. $*P < 0.05$ and $**P < 0.01$. *A*: synergistic enhancement of cell activation by simultaneous addition of 1 μM ACh and 10 μM histamine. The sum of the fluorescence enhancement by addition of ACh or histamine alone calculated separately for each experiment [$\sum(ACh + HA)$] was compared with fluorescence enhancement after simultaneous addition (4th column, $n = 18$). *B*: histamine (10 μM) also enhances the $[Ca^{2+}]_i$ response to ACh when added 10 min earlier ($n = 9$). *C*: the Ca^{2+} ionophore A-23187 (100 nM) did not enhance the $[Ca^{2+}]_i$ response to 10 μM histamine or 1 μM ACh ($n = 12$ and 6, respectively). *D*: histamine (10 μM), but not the histamine 4 receptor (H_4R) agonist 4-methylhistamine (4-mHA, 10 μM), causes cell activation when added alone ($n = 8$, *left*). Activation by histamine is inhibited by preincubation with the histamine 1 receptor (H_1R) inhibitor mepyramine (1 μM, $n = 6$, *right*). *E*: preincubation with the histamine 2 receptor (H_2R) antagonist ranitidine (10 μM) had no significant effect on the $[Ca^{2+}]_i$ response to histamine ($n = 13$). Because cells reacted slowly in this experiment, significance was calculated from measurements taken 20 s after substance addition.

Statistical analysis of $[Ca^{2+}]_i$ imaging experiments. Because it was obvious that increases in fluorescence calculated from the $[Ca^{2+}]_i$ imaging experiments were not normally distributed, statistical significance of the difference of mean values was calculated from ranked data with the unpaired two-tailed *t*-test assuming unequal variances (for a detailed discussion, see Ref. 44). To increase statistical reliability and strength, treatments were always conducted in parallel, resulting in equal sample numbers in each treatment group.

RESULTS

The $[Ca^{2+}]_i$ response to ACh is synergistically enhanced by histamine while histamine alone evokes a small $[Ca^{2+}]_i$ rise via H_1R. P-STS cells reacted with a strong increase in $[Ca^{2+}]_i$ to histamine or the H_4R agonist 4-mHA when added together with a small amount of ACh (44), while histamine or 4-mHA alone did not evoke a significant response in these previous experiments. Here we demonstrate that ACh and histamine in fact acted synergistically in this cell activation when added simultaneously (Fig. 1*A*) and were equally effective when histamine was added 10 min before ACh (Fig. 1*B*). In our previous work (44) we suggested that the observed synergism of ACh and histamine might simply be the result of an elevation of $[Ca^{2+}]_i$ when either compound caused an increased reaction to the second compound. A thorough investigation now showed that the reactions to histamine or ACh alone were not significantly influenced by increasing $[Ca^{2+}]_i$ with the calcium ionophore A-23187 (Fig. 1*C*).

Further experiments showed that 10 μM histamine alone elicited a small rise in $[Ca^{2+}]_i$ not observed with the H_4R agonist 4-mHA alone (Fig. 1*D*, *left*). This reaction, unnoticed in our previous investigations (44), was completely inhibited by the H_1R antagonist mepyramine (Fig. 1*D*, *right*). In our previous work (44) we showed that histamine 3 receptor (H_3R) activation had an inhibitory effect on the $[Ca^{2+}]_i$ response of
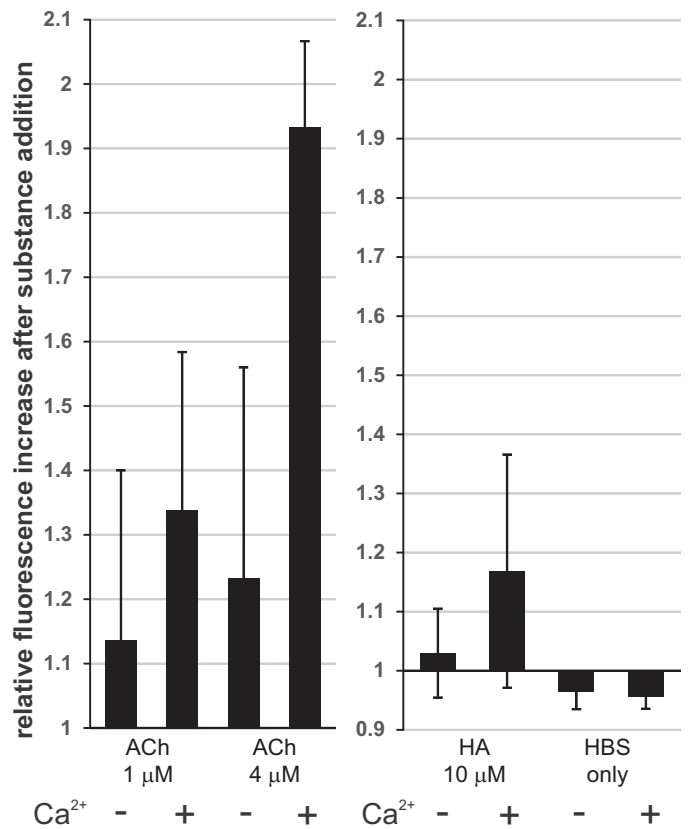
Fig. 3. Influx of external Ca^{2+} contributes to P-STS cell activation by ACh and histamine. The cells were preincubated in HEPES-buffered saline (HBS) with or without 1 mM Ca^{2+} before addition of ACh ($n = 4$) or histamine ($n = 8$) at the indicated concentrations. The intracellular calcium concentration ($[Ca^{2+}]_i$) response of fluo 4-AM-stained P-STS cells was determined as fluorescence enhancement 10 (ACh) or 20 (histamine) s after the start of substance addition in relation to baseline fluorescence. HA, histamine

P-STS cells to ACh, ACh plus histamine, or histamine alone. We did not detect any effect of the histamine 2 receptor (H_2R) antagonist ranitidine on the $[Ca^{2+}]_i$ response of P-STS cells to ACh or ACh plus histamine. Here we tested the effect of ranitidine on cell activation by histamine alone, but again without any significant effect (Fig. 1*E*). In addition, the $[Ca^{2+}]_i$ response of P-STS cells to ACh and epinephrine was compared (Fig. 2). The cells reacted only weakly to a challenge with 100 μM epinephrine while showing a strong response to 1 μM ACh.

T-type VGCCs play a prominent role in the $[Ca^{2+}]_i$ response to ACh and histamine. Experiments conducted in medium prepared without Ca^{2+} indicated a contribution of external Ca^{2+} to the $[Ca^{2+}]_i$ response to ACh or histamine (Fig. 3). To define the pathway of Ca^{2+} influx, several inhibitors of VGCCs were tested for their ability to reduce cell activation by ACh (Fig. 4*A*) and ACh plus histamine (Fig. 4*B*). Inhibitors of L-, N-, P-, and R-type VGCCs {nifedipine [5 μM, IC_{50} ~0.3 μM for L-type channels (50)], ω-conotoxin GVIA, ω-agatoxin IVA, and SNX-482, respectively} had no significant effect, whereas the T-type channel inhibitor mibefradil [5 μM, IC_{50} ~0.3 μM for T-type channels (54)] effectively reduced the increase in $[Ca^{2+}]_i$ in response to ACh and ACh plus histamine. Likewise, only mibefradil inhibited the $[Ca^{2+}]_i$ increase
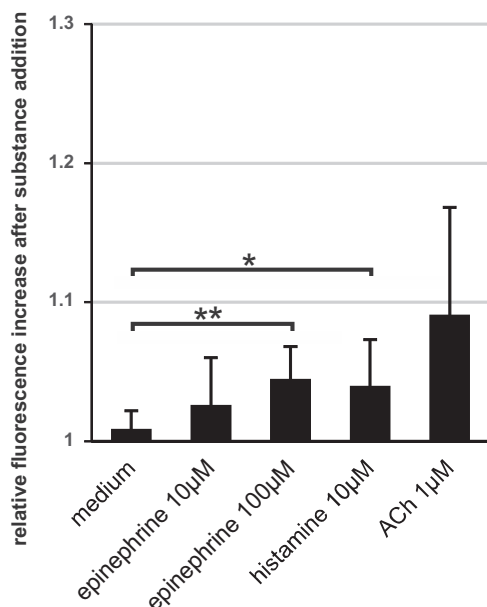

Fig. 2. Comparison of the intracellular calcium concentration ($[Ca^{2+}]_i$) response of P-STS cells to epinephrine, histamine, and ACh. Epinephrine, histamine, or ACh was added to the cells at the indicated concentrations, and the increase in fluo 4-AM fluorescence was determined ($n = 7$). *$P < 0.05$ and **$P < 0.01$.

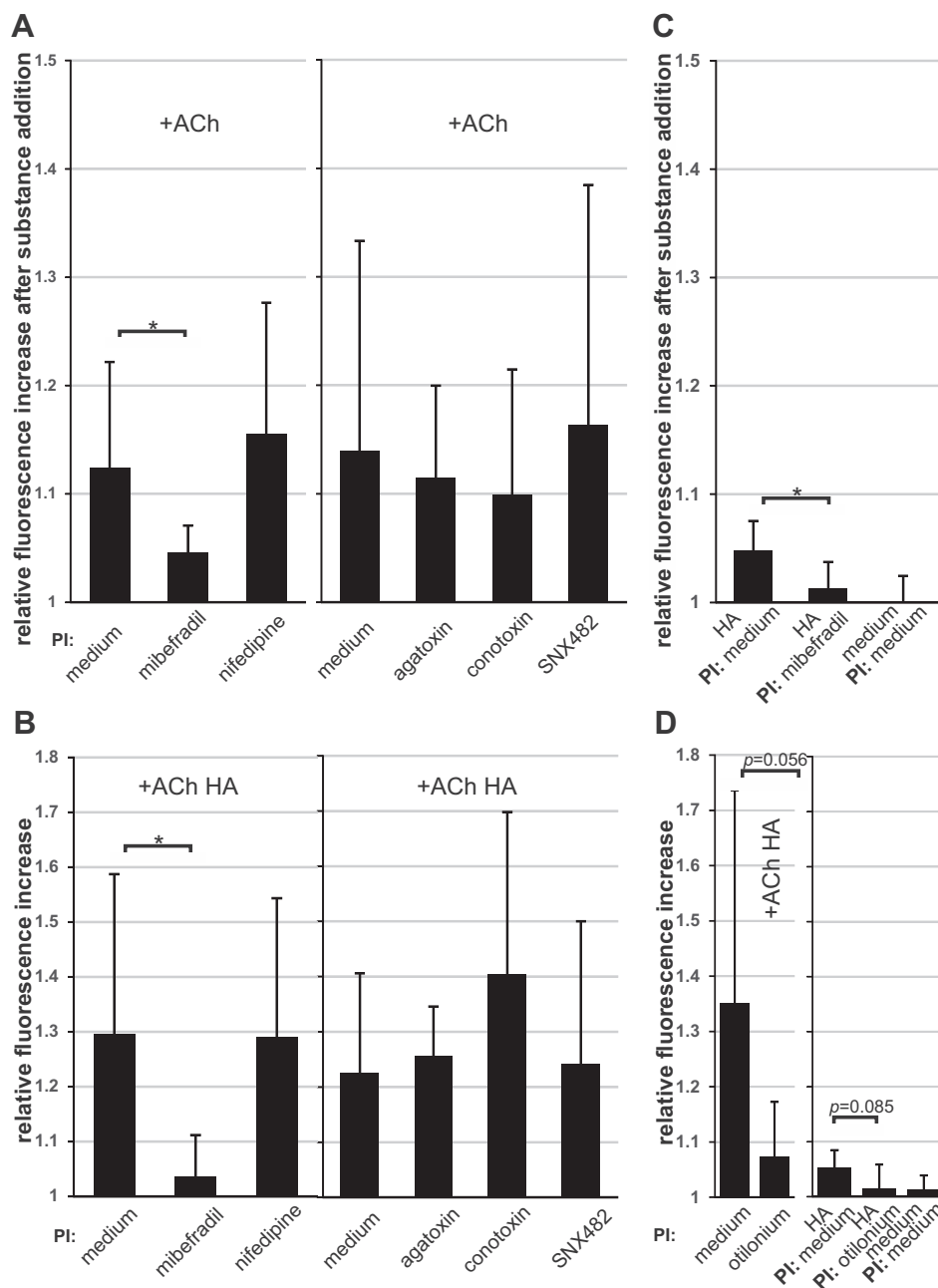Fig. 4. The T-type voltage-gated calcium channel (VGCC) inhibitor mibefradil inhibits the intracellular calcium concentration ($[Ca^{2+}]_i$) response of P-STS cells to ACh, ACh plus histamine, and histamine alone. For preincubation (PI) the indicated substances were added to the cells 10 min before agonist addition. HA, histamine. *$P < 0.05$. *A* and *B*: preincubation with mibefradil (5 μM), but not nifedipine (5 μM), ω-agatoxin IVA (50 nM), ω-conotoxin GVIA (5 nM), or SNX-482 (500 nM), inhibits the $[Ca^{2+}]_i$ response to 1 μM ACh (*A*, *left*: $n = 10$, *right*: $n = 5$) and 1 μM ACh plus 10 μM histamine (*B*, *left*: $n = 8$, *right*: $n = 5$). *C*: preincubation with mibefradil (5 μM) inhibits the $[Ca^{2+}]_i$ response to histamine ($n = 8$). *D*: preincubation with otilonium bromide inhibits the $[Ca^{2+}]_i$ response to 1 μM ACh plus 10 μM histamine ($n = 8$, 1 μM otilonium bromide) and to 10 μM histamine ($n = 10$, 5 μM otilonium bromide). Here the *P* value is slightly higher than 0.05, but, as detailed previously (44), with strong agonists like ACh plus histamine, the applied rank test tends to underestimate significance because of a strongly right-skewed frequency distribution.

induced by histamine alone (Fig. 4*C*), suggesting an important role for T-type channels with all tested agonists without involvement of L-type channels. The participation of P-, N-, and R-type channels in the response to the employed agonists cannot be completely excluded, since the inhibitor concentrations used were rather low to avoid unspecific inhibition. Similar inhibitor concentrations were, however, inhibitory in other systems (4, 42, 51).

An even better inhibitor than mibefradil was the antispasmodic otilonium bromide, an inhibitor of T- and L-type channels (54), but also of muscarinic ACh receptors (35). It already strongly inhibited the $[Ca^{2+}]_i$ response to ACh plus histamine at a concentration of 1 μM. In accordance with its ability to block T-type channels at similar concentrations as mibefradil

(54), otilonium bromide (5 μM) also inhibited the response to histamine alone (Fig. 4*D*).

$[Ca^{2+}]_i$ response to agonists of TRPA1, TRPV1 and TRPV4. A role in visceral nociception has been observed for TRPV1, TRPA1, and TRPV4 (5). Upon stimulation, these channels mediate influx of Ca^{2+} and other cations. We tested the effect of the TRPV1 agonist capsaicin from hot peppers, the TRPA1 agonist cinnamaldehyde from the spice cinnamon, and the TRPV4 agonist GSK-1016790A on P-STS cells in the absence (Fig. 5*A*) and presence (Fig. 5*B*) of ACh, all rendering no significant effects on $[Ca^{2+}]_i$. Piperine, an agonist of TRPV1 and TRPA1 and a constituent in pepper, was also without effect (Fig. 5*A*). Visceral hypersensitivity induced by an agonist of TRPV4 was previously found to be potentiated by
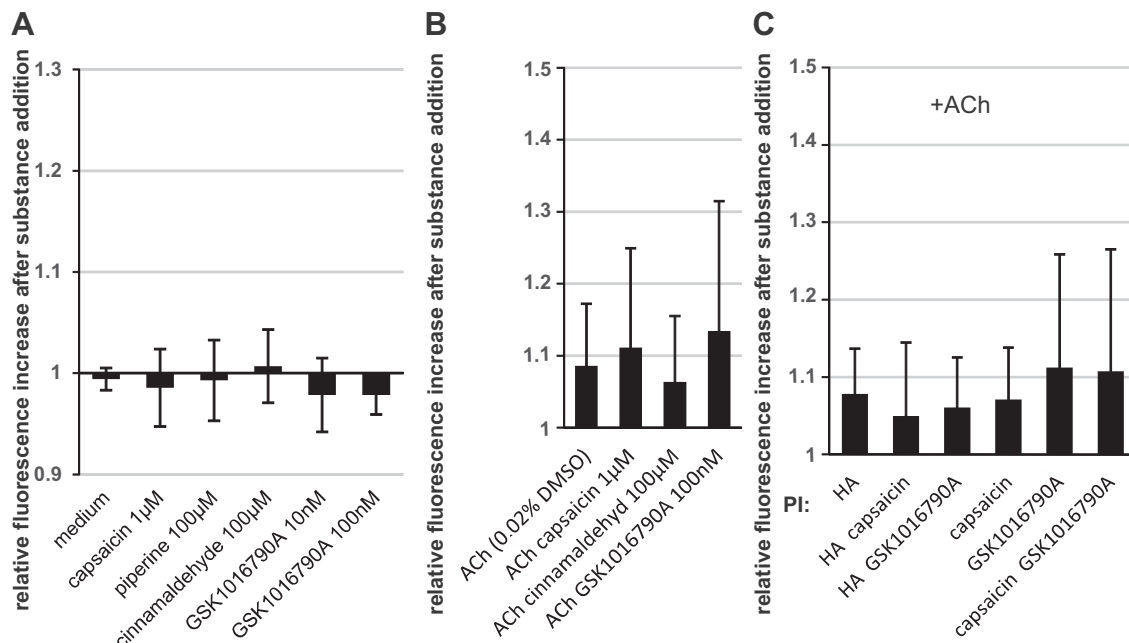
Fig. 5. Effect of transient receptor potential (TRP) channel agonists on the intracellular calcium concentration ($[Ca^{2+}]_i$) response of P-STS cells to ACh, ACh plus histamine, or histamine alone. For preincubation (PI) the indicated substances were added to the cells 10 min before agonist addition. HA, histamine. *A*: no $[Ca^{2+}]_i$ response is detectable with different TRP agonists ($n = 6–8$, final DMSO concentration 0.02% because of preparation of some TRP agonist stocks in DMSO). *B*: no $[Ca^{2+}]_i$ response is detectable with different TRP agonists added together with 1 μM ACh ($n = 7$, final DMSO concentration 0.02%). *C*: combining the transient receptor potential channel vanilloid 1 (TRPV1) agonist capsaicin and the transient receptor potential channel vanilloid 4 (TRPV4) agonist GSK-1016790A with each other or with histamine during preincubation had no discernible effect on the $[Ca^{2+}]_i$ response to ACh. Capsaicin, 50 nM; GSK-1016790A, 100 nM; HA, 2 μM; ACh, 1 μM; $n = 8$.

histamine in vivo and in isolated sensory neurons (14). Likewise, a prominent role of TRPV4 has been seen in cell activation by histamine in human keratinocytes (15), as has a facilitation of GSK-1016790A-induced signaling by TRPV1 in HEK 293 cells expressing TRPV1 and TRPV4 (32). This led us to investigate whether preincubation with different combinations of histamine, capsaicin, and GSK-1016790A had an effect on cell activation by small amounts of ACh (Fig. 5*C*), but no significant enhancement was detected. Notably, in this experiment the histamine concentration was only 2 μM, a concentration that does not always show a clear enhancing effect on the ACh-induced $[Ca^{2+}]_i$ response (also see Ref. 44). This histamine concentration was chosen to allow for further enhancements of $[Ca^{2+}]_i$ by coadded substances.

$[Ca^{2+}]_i$ response to selected nutrient components and degradation products. More important dietary constituents like glutamate, butyrate (a fiber degradation product produced in the intestine), and ATI were tested for their effect on $[Ca^{2+}]_i$ in PSTS cells. None of these compounds caused cell activation when added alone (Fig. 6, *A* and C). The increase in fluorescence upon addition of ATI apparently was because of autofluorescence of ATI, as shown by comparison with ATI added to Hoechst dye 33342-stained fixed cells instead of live fluo 4-AM-stained cells using the same experimental procedure (Fig. 6*C*), and by the fact that, after the initial increase in fluorescence resulting from ATI addition (ATI autofluorescence), there was no further change in fluorescence (Fig. 6*E*). Because ATI have been shown to activate TLR4, the reaction of P-STS cells to the TLR4 ligand LPS was tested for comparison (Fig. 6*C*). Even in the presence of 1% heat-inactivated fetal calf serum, which effectively supplemented components

of the TLR4 signaling pathway in intestinal epithelial cells (13), $[Ca^{2+}]_i$ showed no response to LPS (Fig. 6*D*). Glutamate and butyrate were also added together with ACh (Fig. 6*A*). Although glutamate was without significant effect, butyrate strongly enhanced the response to ACh. In this series of experiments (Fig. 6*A*), the reaction to 1 μM ACh was very weak, which prompted additional experiments. The enhancing effect of butyrate on the response to ACh remained significant (Fig. 6*B*).

Effect of long incubation with histamine, ATI, LPS, or TNF-α on $[Ca^{2+}]_i$ responses to agonists. Because histamine, ATI, or TNF-α are all substances with a suspected role in delayed food-intolerance reactions, IBS, or inflammatory bowel disease (IBD), we further tested whether longer incubation with these substances would have an effect on the susceptibility of P-STS cells to histamine. Preincubation with histamine for 18–20 h before removal of the medium and start of the labeling procedure for $[Ca^{2+}]_i$ imaging appeared to desensitize P-STS cells to histamine, ACh, and ACh plus histamine (Fig. 7*A*). Preincubation with ATI or LPS had no enhancing effect on the response to histamine or ACh plus histamine (Fig. 7, *B* and *C*). After preincubation with TNF-α, implicated in tissue inflammation in IBD, there was still no response to ATI (Fig. 7*E*) or LPS (Fig. 7*D*) but an enhanced response to histamine alone (Fig. 7*D*). The response to ACh plus histamine was too variable to allow any conclusion to be drawn (Fig. 7*D*).

P-STS cells express H_1R, H_4R, FFAR2, FFAR3, TRPV4, and TLR4 mRNA. Our $[Ca^{2+}]_i$ imaging experiments indicated that P-STS cells expressed functional H_1R and H_4R and suggested expression of the short-chain fatty acid receptors FFAR2 or FFAR3 because the cells reacted to butyrate in the presence of
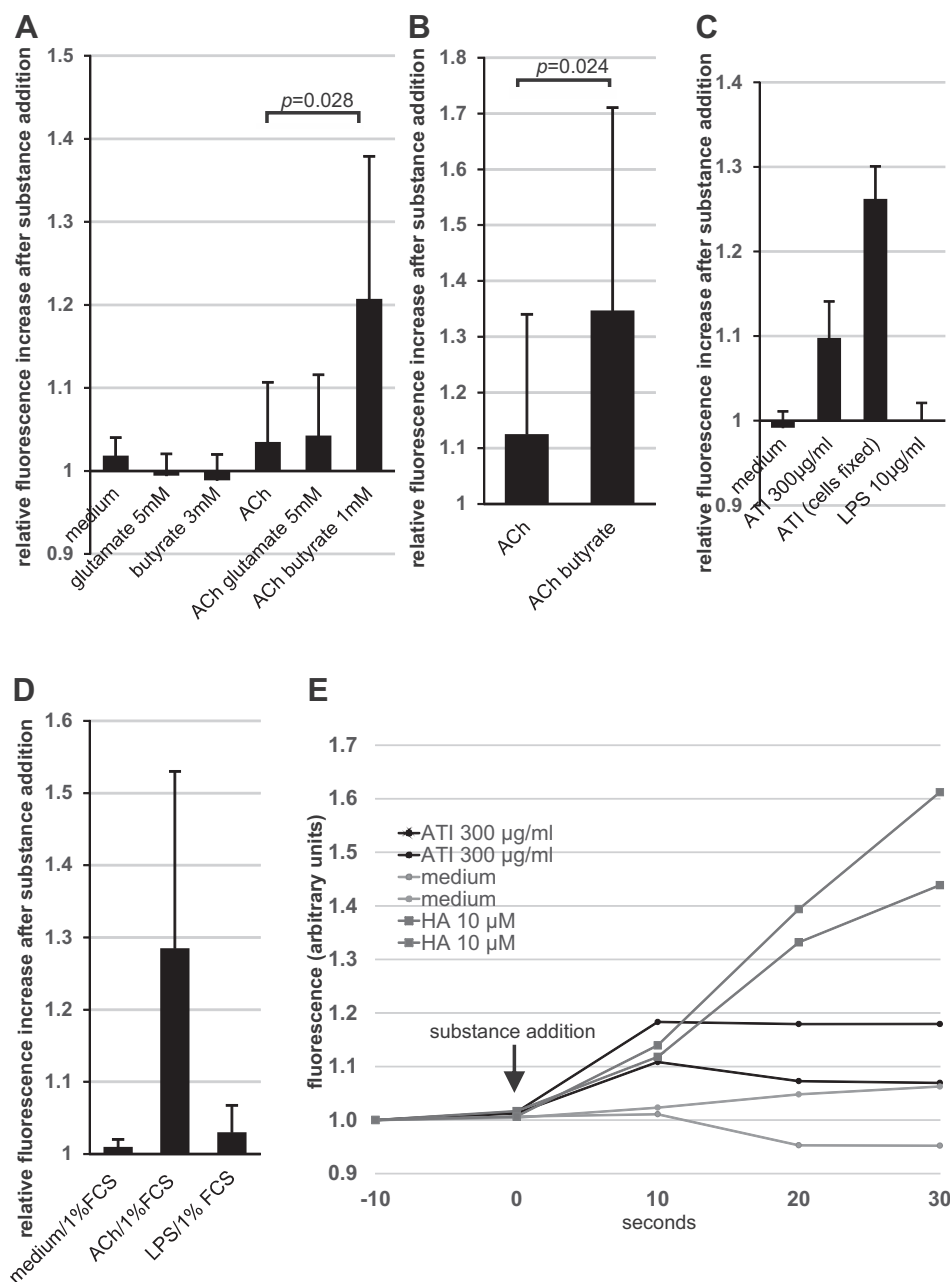
Fig. 6. Effect of selected nutrient components on intracellular calcium concentration ($[Ca^{2+}]_i$) of P-STS cells. *A*: $[Ca^{2+}]_i$ response to glutamate or butyrate added with or without 1 μM ACh ($n = 7$). *B*: $[Ca^{2+}]_i$ response to butyrate (1 or 3 mM) added together with 1 μM ACh ($n = 14$, including the 7 experiments shown in *A*). *C*: fluorescence change upon addition of 300 μg/ml of amylase-trypsin inhibitors (ATI) to live (2nd column, $n = 5$) or fixed (3rd column, $n = 2$) cells or *Escherichia coli* lipopolysaccharide (LPS) to live cells ($n = 6$) showing no difference between the response of live and fixed cells to ATI. *D*: $[Ca^{2+}]_i$ response to LPS in the presence of fetal calf serum (FCS) to supplement potentially missing factors. Heat-inactivated FCS (1% vol/vol) was added to the medium 25 min before substance addition. In this experiment, the $[Ca^{2+}]_i$ response of fluo 4-AM-stained P-STS cells was determined as fluorescence enhancement 20 s after the start of addition of ACh (1 μM, $n = 2$) or LPS (10 μg/ml, $n = 4$) in relation to baseline fluorescence. *E*: time course of fluorescence increase after addition of ATI compared with addition of histamine (HA) or medium. As deduced from *C*, the initial increase in fluorescence after addition of ATI is the result of ATI autofluorescence, but there is no further increase in fluorescence with ATI, indicating a lack of $[Ca^{2+}]_i$ response.

ACh. This was confirmed by detection of the corresponding mRNAs for all of those genes by PCR after reverse transcription (Fig. 8). We also investigated the presence of TRPV4 and TLR4 mRNAs. Although the cells did not respond to the TRPV4 agonist GSK-1016790A or the TLR4 ligand LPS, the mRNAs corresponding to these receptors were expressed (Fig. 8, *lanes 3* and *14*). Sequences for several of the primer pairs used were from the PrimerBank project and were designed to give good results with 40 cycles at 60°C with 1.5 mM $MgCl_2$ and an annealing time of 30 s per cycle. This was confirmed for the TLR4 primer pair ID373432602c1 and the FFAR2 primer pair ID227430361c2 (Fig. 8, *lanes 3* and *5*). With the primer bank primers ID209862766c1 and ID373432602c1 for FFAR3 and TRPV4, respectively, no PCR product was detectable using these conditions (Fig. 8, *lanes 7* and *8*). A PCR product

of FFAR3 with the right size was obtained with the primer pair ID209862766c2, albeit with different cycling conditions (Fig. 8, *lane 10*).

P-STS cells express H_1R, TRPV4, TLR4, and CD14 protein. Protein expression of H_1R, TRPV4, TLR4, and CD14, another component of the LPS receptor (Fig. 9*D*), was verified by immunofluorescence microscopy using blocking peptides or other cell lines as positive or negative controls (Fig. 9).

NF-κB activation after treatment with LPS is undetectable in P-STS cells. Because TLR4 and CD14 protein was detected in P-STS cells but without any $[Ca^{2+}]_i$ response to LPS, we investigated whether LPS treatment would initiate NF-κB signaling in these cells. In addition to nuclear translocation of the p65/RelA subunit of NF-κB in the nucleus after release

Fig. 7. Effect of prolonged incubation of P-STS cells with histamine, amylase-trypsin inhibitors (ATI), lipopolysaccharide (LPS), or tumor necrosis factor-α (TNF-α) on the reactivity to agonists. For preincubation (PI) the indicated substances were added to the cells for 18–20 h, and the medium was exchanged before staining with fluo 4-AM. HA, histamine. If not indicated otherwise, ACh (1 μM), ACh (1 μM) plus histamine (2 μM), histamine (10 μM), LPS (10 μg/ml), or ATI were added to the cells, and the intracellular calcium concentration ($[Ca^{2+}]_i$) response was measured. A: preincubation with histamine ($n = 6$). B: preincubation with ATI ($n = 5$). C: preincubation with LPS (because of high reagibility of the cells only 0.5 μM ACh was added in these experiments, $n = 8$). D: preincubation with 10 ng/ml TNF-α ($n = 6$, except for addition of histamine with $n = 15$). E: time course of fluorescence increase after addition of ATI to cells preincubated with 10 ng/ml TNF-α. As deduced from Fig. 5C, the initial increase in fluorescence after addition of ATI is the result of ATI autofluorescence, but there is no further increase in fluorescence with ATI, indicating a lack of $[Ca^{2+}]_i$ response.
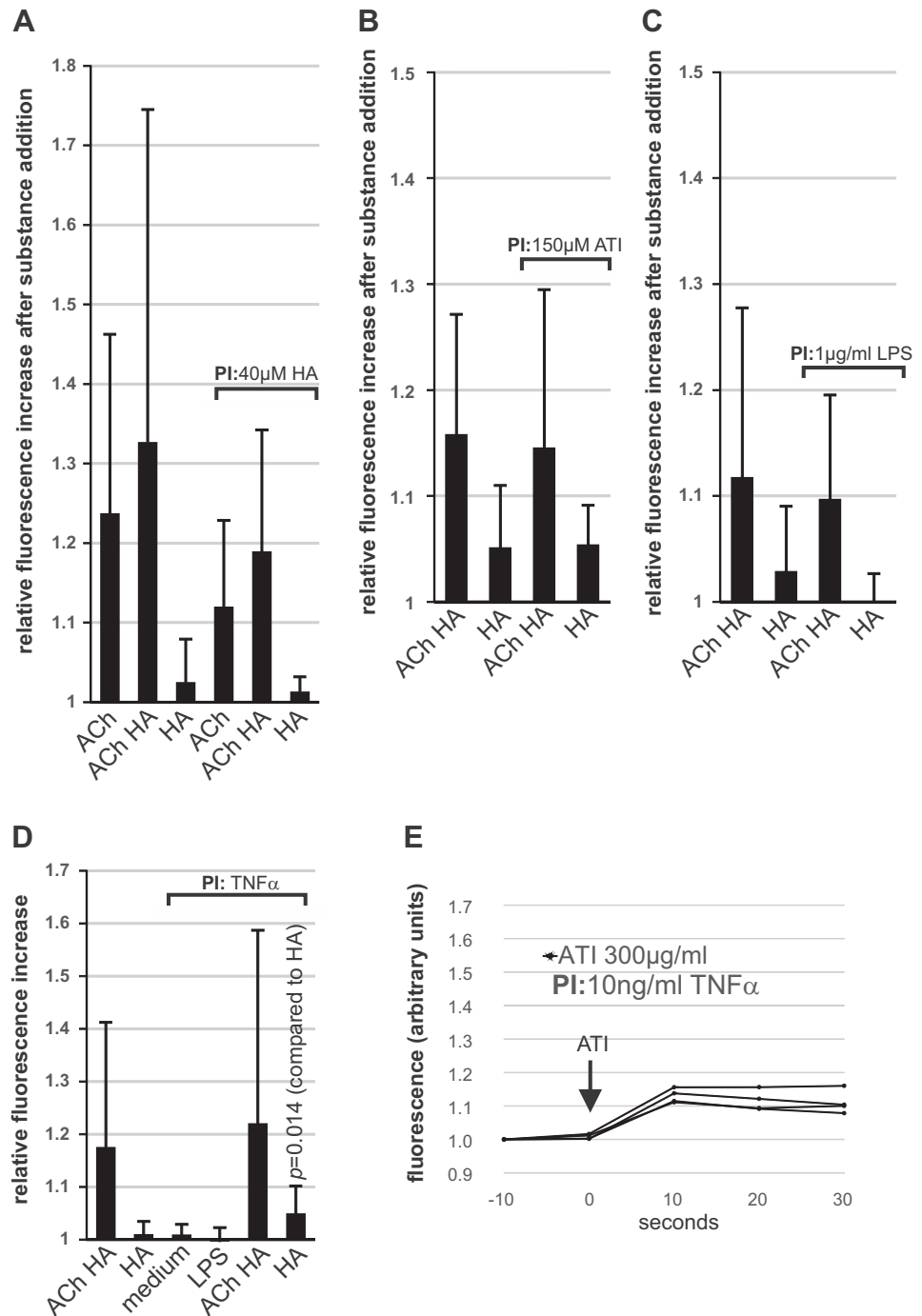
from its complex with cytoplasmic IκB following LPS-induced IκB phosphorylation, LPS is known to induce phosphorylation of Ser[536] of p65 and migration of the phosphorylated protein in the nucleus as an early event of NF-κB activation (39, 66). Immunofluorescence microscopy showed that there was no change in phospho-p65 staining in P-STS cells even after 270 min (Fig. 10B, top) while, in PMA-differentiated THP-1 cells, p65/RelA phosphorylated at Ser[536] migrated from the cytoplasm in the nucleus within 70 min after addition of LPS (Fig. 10A, top). Similarly, p65 distribution remained unchanged in P-STS cells with LPS (Fig. 10B, bottom) while, in control experiments in THP-1 cells, the p65 protein was found primar-

ily in the nucleus 21 h after LPS addition (Fig. 10A, bottom). Treatment of P-STS cells with H_2O_2 for 30 min as a positive control induced migration of p65/RelA in the nucleus (Fig. 10B, bottom).

DISCUSSION

Our work establishes that the previously observed (44) enhancement of the reaction of P-STS cells to ACh by histamine is not only additive but also synergistic. A more thorough investigation of the effect of Ca^{2+} ionophore added to either ACh or histamine alone showed that this synergistic effect
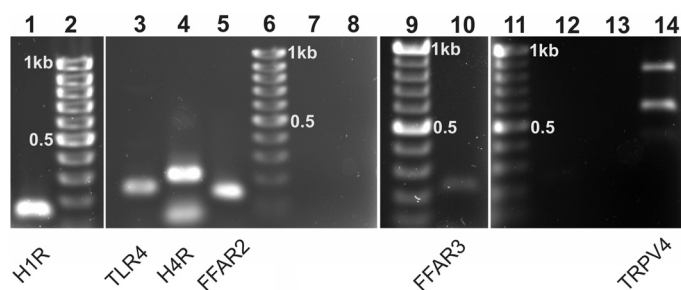
Fig. 8. P-STS cells express histamine 1 receptor (H_1R), histamine 4 receptor (H_4R), free fatty acid receptor 2 (FFAR2), free fatty acid receptor 2 (FFAR3), and transient receptor potential channel vanilloid 4 (TRPV4) mRNA. Detection of mRNAs by reverse transcription-polymerase chain reaction (PCR). *Lanes 7* and *8*, no PCR fragment detectable with the primer bank primers ID209862766c1 and ID373432602c1 for FFAR3 and TRPV4. *Lanes 12* and *13*, no PCR fragment of TRPV4 detectable with 1.5 and 2.0 mM $MgCl_2$ instead of 2.5 mM $MgCl_2$ as used in *lane 14*. TLR4, Toll-like receptor 4.

cannot be explained by a mere rise in $[Ca^{2+}]_i$. The synergistic effect of ACh and histamine is also seen when the cells are preincubated with histamine before addition of ACh. This suggests that pulses of ACh secreted by nerve endings and reaching EC cells located in intestinal crypts could evoke a similar response when histamine concentrations are elevated following mast cell activation. Degranulated mucosal mast cells and elevated histamine levels were detected in patients with IBD and in a subset of IBS patients with increased numbers of intestinal mast cells (reviewed in Refs. 7 and 33). Multiple observations indicate a role of mast cells in gut sensorimotor dysfunction and related diarrhea in IBD and IBS. The susceptibility of P-STS cells to activation by histamine suggests that these symptoms might be partly attributed to increased serotonin release by EC cells in response to elevated histamine secretion by mast cells.

In comparison with the strong response evoked by histamine in the presence of ACh, presumably via H_4R signaling (15), the response to histamine alone appeared weak and may play a minor role in serotonin secretion. Unfortunately, the low serotonin content of P-STS cells does not allow easy detection of secretion (44). Inhibition by the H_1R antagonist mepyramine, a first-generation antihistamine, showed that the $[Ca^{2+}]_i$ response evoked by histamine alone is attributable to H_1R

signaling. The H_4R agonist 4-mHA alone did not cause any significant $[Ca^{2+}]_i$ response. Regarding the other histamine receptors, our previous work has demonstrated that the H_3R agonist methimepip had an inhibitory effect on P-STS activation by ACh, ACh plus histamine, or histamine alone (44). As shown here, the H_2R inhibitor ranitidine did not have any significant effect on the $[Ca^{2+}]_i$ response evoked by histamine. Epinephrine, an agonist sometimes used to stimulate secretion in neuroendocrine cells, evoked only a very weak $[Ca^{2+}]_i$ response in P-STS cells compared with ACh. This is in accordance with the important physiological roles of ACh and serotonin as excitatory stimuli of gut motility (43) and underlines the suitability of the P-STS cell line as a model for intestinal serotonin-secreting cells.

Activation of H_1R by histamine is known to mobilize intracellular Ca^{2+} stores and to cause influx of extracellular Ca^{2+} via voltage-dependent and -independent ion channels in excitable cells (reviewed in Ref. 38). This influx of external calcium is mainly responsible for secretion in response to histamine. The $[Ca^{2+}]_i$ response to histamine, as well as to ACh alone, was also augmented by external Ca^{2+} in P-STS cells.

VGCC are thought to elevate Ca^{2+} locally, and some of them have been shown to interact directly with the secretory machinery (see below). Additional Ca^{2+} entry pathways like TRP channels may trigger or modulate exocytosis (10, 41). We investigated the participation of VGCC in the $[Ca^{2+}]_i$ response of P-STS cells to histamine, ACh, or ACh plus histamine using selective inhibitors for L-, N-, P-, R-, and T-type VGCC. Only the T-type channel inhibitor mibefradil showed a significant inhibitory effect. Mibefradil inhibited the $[Ca^{2+}]_i$ response for histamine alone and for ACh and ACh plus histamine. In contrast to the other VGCC channels mentioned, T-type VGCC are low-voltage-activated channels that ensure secretion at membrane potentials near the resting conditions important for basal hormone release or sustained release during mild stimulations (reviewed in Refs. 12 and 63). There is ample evidence for their participation in neurotransmitter release in neuroendocrine cells, although they lack the consensus synaptic protein interaction (synprint) site allowing N- and P/Q-type VGCC to bind proteins of the secretion machinery. An increased density of T-type VGCC is seen as a response to stressors in many cells and tissues, presumably lowering the action potential firing
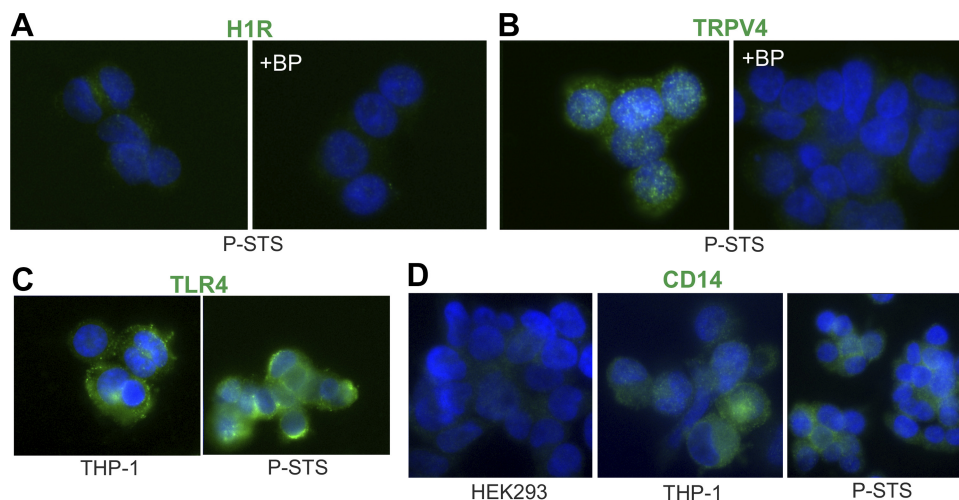

Fig. 9. P-STS cells express histamine 1 receptor (H_1R), transient receptor potential channel vanilloid 4 (TRPV4), Toll-like receptor 4 (TLR4), and CD14 protein. *A* and *B*: immunofluorescence staining of P-STS cells with anti-H_1R (*A*) or anti-TRPV4 (*B*) in the presence (+BP) or absence of the corresponding blocking peptide and detected with goat Alexa 488-labeled secondary antibodies (green). *C*: immunofluorescence staining of P-STS cells and phorbol 12-myristate,13-acetate (PMA)-differentiated THP-1 monocytes/macrophages with anti-TLR4 detected with goat Alexa 488-labeled secondary antibody (green). *D*: immunofluorescence staining of P-STS cells, HEK 293 cells (supposed to have no CD14) (18), and PMA-differentiated THP-1 monocytes/macrophages with anti-CD14 detected with goat Alexa 488-labeled secondary antibody (green). Blue, nuclei.
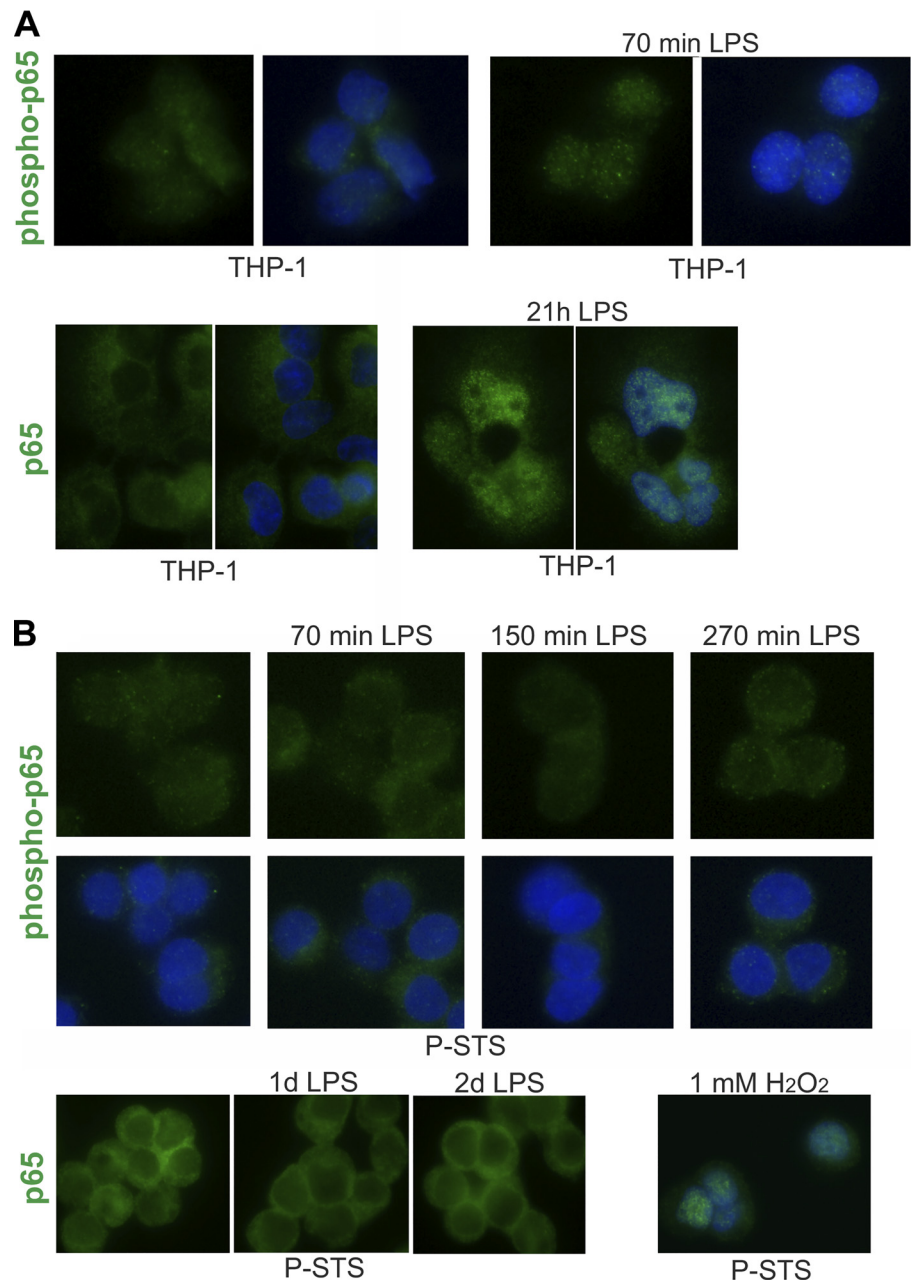
Fig. 10. The p65/RelA protein in P-STS cells shows no reaction to lipopolysaccharide (LPS). Phorbol 12-myristate,13-acetate (PMA)-differentiated THP-1 monocytes/macrophages (*A*) or P-STS (*B*) cells were grown on cover glass slides, washed with pure medium, and incubated for 30 min at 37°C in 200 μl of medium containing 1% heat-inactivated fetal calf serum (FCS) (phospho-NF-κB p65) or in 400 μl full medium (NF-κB p65). LPS (1 μg/ml) was added, and the cells were either fixed immediately or further incubated at 37°C for the indicated time before fixation and staining for immunofluorescence with phospho-NF-κB p65(Ser^{536}) or RelA/NF-κB p65 detected with a goat Alexa 488-labeled secondary antibody (green). Merged images with nuclear staining (blue) are shown for THP-1 cells and phospho-p65-labeled P-STS cells. As a positive control for migration of P-STS NF-κB p65 in the nucleus, the cells were treated with 1 mM H$_2$O$_2$ in complete medium for 30 min and further incubated in medium without H$_2$O$_2$ for 3 h (*B*, 2nd row, *right*).

threshold (12). Thus, the importance of T-type VGCC for histamine-induced and ACh-induced cell activation in P-STS cells may be a typical feature of human EC cells. T-type channel blockers have been suggested as promising candidates for novel analgesics potentially useful for treating visceral pain and discomfort (3). Otilonium bromide, a spasmolytic with significant therapeutic effect in IBS and minimal systemic absorption from the intestine (3, 11, 16, 59), is known to inhibit T- and L-type VGCC and muscarinic ACh receptors (27, 31). Accordingly, otilonium bromide effectively inhibited the synergistic enhancement of the [Ca^{2+}]$_i$ response to ACh by histamine and the response to histamine alone, confirming the results with mibefradil. This suggests that otilonium bromide might be useful not only in IBS but also in histamine intolerance and food allergy by obviating excessive dietary restrictions that might have detrimental effects.

A role in visceral nociception and hypersensitivity, an important clinical problem for the patients, has been suggested for TRPA1, TRPV1, and TRPV4 (5, 37). Accordingly, agonists of these cation channels, including the food constituents capsaicin, cinnamaldehyde, and piperine, were tested for their effect on the [Ca^{2+}]$_i$ response of P-STS cells in the absence or presence of ACh, histamine, or both agonists. These experiments gave no indication of the presence of functional TRPA1, TRPV1, or TRPV4. Because there is evidence suggesting that TRPV4 expression is increased in the intestine of IBS patients and that in these patients elevated levels of histamine and serotonin are implicated in the development of visceral hypersensitivity (reviewed in Refs. 23 and 64), we looked for expression of TRPV4 in P-STS cells. We detected both TRPV4 mRNA and protein. Further research will be necessary to clarify why the cells do not react to the TRPV4 agonist

GSK-1016790A. Possible explanations include low TRPV4 localization at the cell surface or expression of nonfunctional TRPV4. In this respect, it is interesting that, in primary human endothelial cells, most TRPV4 channels remained silent even during maximal stimulation with GSK-1016790A (56).

There was a weak $[Ca^{2+}]_i$ response with butyrate when added together with ACh. Induction of serotonin secretion by butyrate would be consistent with the necessity for increased gut motility when microbial activity is high to pursue digestion and prevent bacterial overgrowth in the small intestine (52). Short-chain fatty acid concentrations of 70–140 mM have been observed in the proximal colon (65), and about one-tenth of this concentration was found in human ileum (17). Short-chain fatty acids are agonists of the free fatty acid receptors FFAR2/G protein-coupled receptor 43 and FFAR3/G protein-coupled receptor 41 and induced a $[Ca^{2+}]_i$ response when transfected in Chinese hamster ovary cells (34). They are involved in hormone secretion by intestinal neuroendocrine cells (8). Butyrate and FFAR2 have been implicated in serotonin secretion by neuroendocrine cells (2, 47). We show that P-STS cells express mRNA of both FFAR2 and FFAR3.

Upon addition of glutamate, glutamate plus ACh, or ATI, there was no $[Ca^{2+}]_i$ response in P-STS cells. Because the IL-8 response to ATI in human monocyte-derived dendritic cells depends heavily on TLR4 and CD14 (28), we tested the response of P-STS cells to LPS, another ligand of the TLR4-MD-2-CD14 complex. Despite the presence of TLR4 and CD14 protein confirmed by immunofluorescence microscopy, the cells showed neither a $[Ca^{2+}]_i$ response to LPS nor discernible migration of NF-κB p65/RelA or Ser[536]-phosphorylated p65/RelA to the nucleus. Whereas preincubation with TNF-α simulating inflammatory conditions considerably increased the $[Ca^{2+}]_i$ response to histamine alone, long-term incubation with ATI or LPS had no such effect. No protein-altering insertions/deletions or rare single nucleotide polymorphisms have been found in the P-STS TLR4 sequence (27). It is unknown, however, whether P-STS cells express MD-2, which was critical for LPS responses in intestinal epithelial cell lines and a CHO cell line (1, 49). In accordance with our results, in a previous study, LPS evoked only an insignificant release of serotonin in human EC cells isolated from normal mucosa, whereas in EC cells from Crohn's colitis mucosa, there was an increased serotonin secretion in response to LPS (31). Control of signaling to commensal microorganisms is extremely important in the intestinal epithelium. Low expression of Toll-like receptors and accessory proteins may be a means of avoiding hyperresponsiveness (61) (reviewed in Refs. 40 and 58). Additional control mechanisms of TLR signaling include location of TLRs in intracellular compartments or at the basolateral membrane and negative regulation of signaling by inhibitory factors. An investigation into the complexity of this regulatory network in P-STS cells would exceed the scope of this work.

Recent evidence indicates that LPS can directly activate the cation channels TRPA1 and TRPV4 and induce an increase in $[Ca^{2+}]_i$ (9). Interaction of LPS with TLR4 has been shown to sensitize TRPV1 to capsaicin (37). These properties of LPS might be the physiological reason for the lack of functional TRPA1, TRPV1, and TRPV4 in P-STS cells, since constant exposition to LPS of cells exposed to the gut lumen otherwise might activate these channels.

In conclusion, in this work, we show work that, in addition to H_3R and H_4R, P-STS ileal EC cells express the H_1R and are also sensitive to histamine in the absence of ACh. Histamine and ACh together cause a synergistic increase in $[Ca^{2+}]_i$ that is inhibited by the spasmolytic otilonium bromide, a drug ameliorating symptoms in IBS. Otilonium bromide also inhibits cell activation by histamine alone. These results suggest that it might be therapeutically useful in histamine intolerance and food allergy. Our data indicate that the T-type VGCCs participate in the increase in $[Ca^{2+}]_i$ evoked by histamine, which is a requirement for serotonin secretion. Pretreatment with TNF-α considerably increased the $[Ca^{2+}]_i$ response to histamine alone, suggesting that patients with IBD or IBS with a tendency toward inflammation might have increased susceptibility to histamine and activation of mast cells. The cells showed no response to wheat amylase-trypsin inhibitors, suggesting that EC cells are not directly involved in nongluten wheat sensitivity.

DISCLOSURES

No conflicts of interest, financial or otherwise, are declared by the authors.

AUTHOR CONTRIBUTIONS

B.P. and E.J.-J. conceived and designed research; B.P. and V.F.Z. performed experiments; B.P. analyzed data; B.P., V.F.Z., D.S., and E.J.-J. interpreted results of experiments; B.P. prepared figures; B.P. drafted manuscript; B.P., V.F.Z., D.S., R.P., and E.J.-J. approved final version of manuscript; V.F.Z., D.S., R.P., and E.J.-J. edited and revised manuscript.

REFERENCES

1. **Abreu MT, Vora P, Faure E, Thomas LS, Arnold ET, Arditi M.** Decreased expression of Toll-like receptor-4 and MD-2 correlates with intestinal epithelial cell protection against dysregulated proinflammatory gene expression in response to bacterial lipopolysaccharide. *J Immunol* 167: 1609–1616, 2001. doi:10.4049/jimmunol.167.3.1609.

2. **Akiba Y, Inoue T, Kaji I, Higashiyama M, Narimatsu K, Iwamoto K, Watanabe M, Guth PH, Engel E, Kuwahara A, Kaunitz JD.** Short-chain fatty acid sensing in rat duodenum. *J Physiol* 593: 585–599, 2015. doi:10.1113/jphysiol.2014.280792.

3. **Annaházi A, Róka R, Rosztóczy A, Wittmann T.** Role of antispasmodics in the treatment of irritable bowel syndrome. *World J Gastroenterol* 20: 6031–6043, 2014. doi:10.3748/wjg.v20.i20.6031.

4. **Arroyo G, Aldea M, Fuentealba J, Albillos A, García AG.** SNX482 selectively blocks P/Q Ca2+ channels and delays the inactivation of Na+ channels of chromaffin cells. *Eur J Pharmacol* 475: 11–18, 2003. doi:10.1016/S0014-2999(03)02084-3.

5. **Beckers AB, Weerts ZZ, Helyes Z, Masclee AA, Keszthelyi D.** Review article: transient receptor potential channels as possible therapeutic targets in irritable bowel syndrome. *Aliment Pharmacol Ther* 46: 938–952, 2017. doi:10.1111/apt.14294.

6. **Bertrand PP, Bertrand RL.** Serotonin release and uptake in the gastrointestinal tract. *Auton Neurosci* 153: 47–57, 2010. doi:10.1016/j.autneu.2009.08.002.

7. **Bischoff SC.** Physiological and pathophysiological functions of intestinal mast cells. *Semin Immunopathol* 31: 185–205, 2009. doi:10.1007/s00281-009-0165-4.

8. **Bolognini D, Tobin AB, Milligan G, Moss CE.** The pharmacology and function of receptors for short-chain fatty acids. *Mol Pharmacol* 89: 388–398, 2016. doi:10.1124/mol.115.102301.

9. **Boonen B, Alpizar YA, Sanchez A, López-Requena A, Voets T, Talavera K.** Differential effects of lipopolysaccharide on mouse sensory TRP channels. *Cell Calcium* 73: 72–81, 2018. doi:10.1016/j.ceca.2018.04.004.

10. **Calvo-Gallardo E, López-Gil Á, Méndez-López I, Martínez-Ramírez C, Padín JF, García AG.** Faster kinetics of quantal catecholamine release in mouse chromaffin cells stimulated with acetylcholine, compared with other secretagogues. *J Neurochem* 139: 722–736, 2016. doi:10.1111/jnc.13849.

11. **Camilleri M, Boeckxstaens G.** Dietary and pharmacological treatment of abdominal pain in IBS. *Gut* 66: 966–974, 2017. doi:10.1136/gutjnl-2016-313425.

12. **Carbone E, Calorio C, Vandael DH.** T-type channel-mediated neurotransmitter release. *Pflugers Arch* 466: 677–687, 2014. doi:10.1007/s00424-014-1489-z.

13. **Cario E, Rosenberg IM, Brandwein SL, Beck PL, Reinecker HC, Podolsky DK.** Lipopolysaccharide activates distinct signaling pathways in intestinal epithelial cell lines expressing Toll-like receptors. *J Immunol* 164: 966–972, 2000. doi:10.4049/jimmunol.164.2.966.

14. **Cenac N, Altier C, Motta JP, d'Aldebert E, Galeano S, Zamponi GW, Vergnolle N.** Potentiation of TRPV4 signalling by histamine and serotonin: an important mechanism for visceral hypersensitivity. *Gut* 59: 481–488, 2010. doi:10.1136/gut.2009.192567.

15. **Chen Y, Fang Q, Wang Z, Zhang JY, MacLeod AS, Hall RP, Liedtke WB.** Transient receptor potential vanilloid 4 ion channel functions as a pruriceptor in epidermal keratinocytes to evoke histaminergic itch. *J Biol Chem* 291: 10252–10262, 2016. doi:10.1074/jbc.M116.716464.

16. **Clavé P, Tack J.** Efficacy of otilonium bromide in irritable bowel syndrome: a pooled analysis. *Therap Adv Gastroenterol* 10: 311–322, 2017. doi:10.1177/1756283X16681708.

17. **Cummings JH, Pomare EW, Branch WJ, Naylor CP, Macfarlane GT.** Short chain fatty acids in human large intestine, portal, hepatic and venous blood. *Gut* 28: 1221–1227, 1987. doi:10.1136/gut.28.10.1221.

18. **Divanovic S, Trompette A, Atabani SF, Madan R, Golenbock DT, Visintin A, Finberg RW, Tarakhovsky A, Vogel SN, Belkaid Y, Kurt-Jones EA, Karp CL.** Negative regulation of Toll-like receptor 4 signaling by the Toll-like receptor homolog RP105. *Nat Immunol* 6: 571–578, 2005. doi:10.1038/ni1198.

19. **Diwakarla S, Fothergill LJ, Fakhry J, Callaghan B, Furness JB.** Heterogeneity of enterochromaffin cells within the gastrointestinal tract. *Neurogastroenterol Motil* 29: 6, 2017. doi:10.1111/nmo.13101.

20. **Gershon MD.** 5-Hydroxytryptamine (serotonin) in the gastrointestinal tract. *Curr Opin Endocrinol Diabetes Obes* 20: 14–21, 2013. doi:10.1097/MED.0b013e32835bc703.

21. **Gershon MD.** Nerves, reflexes, and the enteric nervous system: pathogenesis of the irritable bowel syndrome. *J Clin Gastroenterol* 39, *Suppl* 3: S184–S193, 2005. doi:10.1097/01.mcg.0000156403.37240.30.

22. **Glassmeier G, Strübing C, Riecken EO, Buhr H, Neuhaus P, Ahnert-Hilger G, Wiedenmann B, Scherübl H.** Electrophysiological properties of human carcinoid cells of the gut. *Gastroenterology* 113: 90–100, 1997. doi:10.1016/S0016-5085(97)70084-2.

23. **Grace MS, Bonvini SJ, Belvisi MG, McIntyre P.** Modulation of the TRPV4 ion channel as a therapeutic target for disease. *Pharmacol Ther* 177: 9–22, 2017. doi:10.1016/j.pharmthera.2017.02.019.

24. **Grozinsky-Glasberg S, Shimon I, Rubinfeld H.** The role of cell lines in the study of neuroendocrine tumors. *Neuroendocrinology* 96: 173–187, 2012. doi:10.1159/000338793.

25. **Hansen MB, Witte AB.** The role of serotonin in intestinal luminal sensing and secretion. *Acta Physiol (Oxf)* 193: 311–323, 2008. doi:10.1111/j.1748-1716.2008.01870.x.

26. **Harrington AM, Hutson JM, Southwell BR.** Cholinergic neurotransmission and muscarinic receptors in the enteric nervous system. *Prog Histochem Cytochem* 44: 173–202, 2010. doi:10.1016/j.proghi.2009.10.001.

27. **Hofving T, Arvidsson Y, Almobarak B, Inge L, Pfragner R, Persson M, Stenman G, Kristiansson E, Johanson V, Nilsson O.** The neuroendocrine phenotype, genomic profile and therapeutic sensitivity of GEP-NET cell lines. *Endocr Relat Cancer* 25: 367–380, 2018. doi:10.1530/ERC-17-0445.

28. **Junker Y, Zeissig S, Kim SJ, Barisani D, Wieser H, Leffler DA, Zevallos V, Libermann TA, Dillon S, Freitag TL, Kelly CP, Schuppan D.** Wheat amylase trypsin inhibitors drive intestinal inflammation via activation of toll-like receptor 4. *J Exp Med* 209: 2395–2408, 2012. doi:10.1084/jem.20102660.

29. **Kendig DM, Grider JR.** Serotonin and colonic motility. *Neurogastroenterol Motil* 27: 899–905, 2015. doi:10.1111/nmo.12617.

30. **Khan WI, Ghia JE.** Gut hormones: emerging role in immune activation and inflammation. *Clin Exp Immunol* 161: 19–27, 2010. doi:10.1111/j.1365-2249.2010.04150.x.

31. **Kidd M, Gustafsson BI, Drozdov I, Modlin IM.** IL1beta- and LPS-induced serotonin secretion is increased in EC cells derived from Crohn's disease. *Neurogastroenterol Motil* 21: 439–450, 2009. doi:10.1111/j.1365-2982.2008.01210.x.

32. **Kim S, Barry DM, Liu XY, Yin S, Munanairi A, Meng QT, Cheng W, Mo P, Wan L, Liu SB, Ratnayake K, Zhao ZQ, Gautam N, Zheng J, Karunarathne WK, Chen ZF.** Facilitation of TRPV4 by TRPV1 is required for itch transmission in some sensory neuron populations. *Sci Signal* 9: ra71, 2016. doi:10.1126/scisignal.aaf1047.

33. **Lee KN, Lee OY.** The role of mast cells in irritable bowel syndrome. *Gastroenterol Res Pract* 2016: 2031480, 2016. doi:10.1155/2016/2031480.

34. **Le Poul E, Loison C, Struyf S, Springael JY, Lannoy V, Decobecq ME, Brezillon S, Dupriez V, Vassart G, Van Damme J, Parmentier M, Detheux M.** Functional characterization of human receptors for short chain fatty acids and their role in polymorphonuclear cell activation. *J Biol Chem* 278: 25481–25489, 2003. doi:10.1074/jbc.M301403200.

35. **Lindqvist S, Hernon J, Sharp P, Johns N, Addison S, Watson M, Tighe R, Greer S, Mackay J, Rhodes M, Lewis M, Stebbings W, Speakman C, Evangelista S, Johnson I, Williams M.** The colon-selective spasmolytic otilonium bromide inhibits muscarinic M(3) receptor-coupled calcium signals in isolated human colonic crypts. *Br J Pharmacol* 137: 1134–1142, 2002. doi:10.1038/sj.bjp.0704942.

36. **Lomax AE, Linden DR, Mawe GM, Sharkey KA.** Effects of gastrointestinal inflammation on enteroendocrine cells and enteric neural reflex circuits. *Auton Neurosci* 126–127: 250–257, 2006. doi:10.1016/j.autneu.2006.02.015.

37. **Lopez-Requena A, Boonen B, Van Gerven L, Hellings PW, Alpizar YA, Talavera K.** Roles of neuronal TRP channels in neuroimmune interactions. In: *Neurobiology of TRP Channels*, edited by Emir TLR. Boca Raton, FL: CRC, 2017, p. 277–294.

38. **Marley PD.** Mechanisms in histamine-mediated secretion from adrenal chromaffin cells. *Pharmacol Ther* 98: 1–34, 2003. doi:10.1016/S0163-7258(03)00002-0.

39. **Mattioli I, Sebald A, Bucher C, Charles RP, Nakano H, Doi T, Kracht M, Schmitz ML.** Transient and selective NF-kappa B p65 serine 536 phosphorylation induced by T cell costimulation is mediated by I kappa B kinase beta and controls the kinetics of p65 nuclear import. *J Immunol* 172: 6336–6344, 2004. doi:10.4049/jimmunol.172.10.6336.

40. **McClure R, Massari P.** TLR-dependent human mucosal epithelial cell responses to microbial pathogens. *Front Immunol* 5: 386, 2014. doi:10.3389/fimmu.2014.00386.

41. **Obukhov AG, Nowycky MC.** TRPC4 can be activated by G-protein-coupled receptors and provides sufficient Ca(2+) to trigger exocytosis in neuroendocrine cells. *J Biol Chem* 277: 16172–16178, 2002. doi:10.1074/jbc.M111664200.

42. **O'Farrell M, Marley PD.** Different contributions of voltage-sensitive Ca2+ channels to histamine-induced catecholamine release and tyrosine hydroxylase activation in bovine adrenal chromaffin cells. *Cell Calcium* 25: 209–217, 1999. doi:10.1054/ceca.1999.0025.

43. **Olsson C, Holmgren S.** The control of gut motility. *Comp Biochem Physiol A Mol Integr Physiol* 128: 481–503, 2001. doi:10.1016/S1095-6433(00)00330-5.

44. **Pfanzagl B, Mechtcheriakova D, Meshcheryakova A, Aberle SW, Pfragner R, Jensen-Jarolim E.** Activation of the ileal neuroendocrine tumor cell line P-STS by acetylcholine is amplified by histamine: role of H3R and H4R. *Sci Rep* 7: 1313, 2017. doi:10.1038/s41598-017-01453-5.

45. **Pfragner R, Behmel A, Höger H, Beham A, Ingolic E, Stelzer I, Svejda B, Moser VA, Obenauf AC, Siegl V, Haas O, Niederle B.** Establishment and characterization of three novel cell lines - P-STS, L-STS, H-STS - derived from a human metastatic midgut carcinoid. *Anticancer Res* 29: 1951–1961, 2009.

46. **Raghupathi R, Duffield MD, Zelkas L, Meedeniya A, Brookes SJ, Sia TC, Wattchow DA, Spencer NJ, Keating DJ.** Identification of unique release kinetics of serotonin from guinea-pig and human entero-

chromaffin cells. *J Physiol* 591: 5959–5975, 2013. doi:10.1113/jphysiol.2013.259796.

47. **Reigstad CS, Salmonson CE, Rainey JF III, Szurszewski JH, Linden DR, Sonnenburg JL, Farrugia G, Kashyap PC.** Gut microbes promote colonic serotonin production through an effect of short-chain fatty acids on enterochromaffin cells. *FASEB J* 29: 1395–1403, 2015. doi:10.1096/fj.14-259598.

48. **Rinner B, Gallè B, Trajanoski S, Fischer C, Hatz M, Maierhofer T, Michelitsch G, Moinfar F, Stelzer I, Pfragner R, Guelly C.** Molecular evidence for the bi-clonal origin of neuroendocrine tumor derived metastases. *BMC Genomics* 13: 594, 2012. doi:10.1186/1471-2164-13-594.

49. **Schromm AB, Lien E, Henneke P, Chow JC, Yoshimura A, Heine H, Latz E, Monks BG, Schwartz DA, Miyake K, Golenbock DT.** Molecular genetic analysis of an endotoxin nonresponder mutant cell line: a point mutation in a conserved region of MD-2 abolishes endotoxin-induced signaling. *J Exp Med* 194: 79–88, 2001. doi:10.1084/jem.194.1.79.

50. **Shen JB, Jiang B, Pappano AJ.** Comparison of L-type calcium channel blockade by nifedipine and/or cadmium in guinea pig ventricular myocytes. *J Pharmacol Exp Ther* 294: 562–570, 2000.

51. **Sidach SS, Mintz IM.** Low-affinity blockade of neuronal N-type Ca channels by the spider toxin omega-agatoxin-IVA. *J Neurosci* 20: 7174–7182, 2000. doi:10.1523/JNEUROSCI.20-19-07174.2000.

52. **Šket R, Treichel N, Debevec T, Eiken O, Mekjavic I, Schloter M, Vital M, Chandler J, Tiedje JM, Murovec B, Prevoršek Z, Stres B.** Hypoxia and inactivity related physiological changes (constipation, inflammation) are not reflected at the level of gut metabolites and butyrate producing microbial community: the PlanHab study. *Front Physiol* 8: 250, 2017. doi:10.3389/fphys.2017.00250.

53. **Spandidos A, Wang X, Wang H, Seed B.** PrimerBank: a resource of human and mouse PCR primer pairs for gene expression detection and quantification. *Nucleic Acids Res* 38, *Suppl* 1: D792–D799, 2010. doi:10.1093/nar/gkp1005.

54. **Strege PR, Sha L, Beyder A, Bernard CE, Perez-Reyes E, Evangelista S, Gibbons SJ, Szurszewski JH, Farrugia G.** T-type Ca(2+) channel modulation by otilonium bromide. *Am J Physiol Gastrointest Liver Physiol* 298: G706–G713, 2010. doi:10.1152/ajpgi.00437.2009.

55. **Sugata Y, Okano M, Fujiwara T, Matsumoto R, Hattori H, Yamamoto M, Nishibori M, Nishizaki K.** Histamine H4 receptor agonists have more activities than H4 agonism in antigen-specific human T-cell responses. *Immunology* 121: 266–275, 2007. doi:10.1111/j.1365-2567.2007.02574.x.

56. **Sullivan MN, Francis M, Pitts NL, Taylor MS, Earley S.** Optical recording reveals novel properties of GSK1016790A-induced vanilloid transient receptor potential channel TRPV4 activity in primary human endothelial cells. *Mol Pharmacol* 82: 464–472, 2012. doi:10.1124/mol.112.078584.

57. **Tan J, McKenzie C, Potamitis M, Thorburn AN, Mackay CR, Macia L.** The role of short-chain fatty acids in health and disease. *Adv Immunol* 121: 91–119, 2014. doi:10.1016/B978-0-12-800100-4.00003-9.

58. **Tan Y, Zanoni I, Cullen TW, Goodman AL, Kagan JC.** Mechanisms of Toll-like receptor 4 endocytosis reveal a common immune-evasion strategy used by pathogenic and commensal bacteria. *Immunity* 43: 909–922, 2015. doi:10.1016/j.immuni.2015.10.008.

59. **Triantafillidis JK, Malgarinos G.** Long-term efficacy and safety of otilonium bromide in the management of irritable bowel syndrome: a literature review. *Clin Exp Gastroenterol* 7: 75–82, 2014. doi:10.2147/CEG.S46291.

60. **Turvill JL, Farthing MJ.** Role of the neuroendocrine system in pathogenesis of gastroenteritis. *Curr Opin Infect Dis* 13: 523–529, 2000. doi:10.1097/00001432-200010000-00015.

61. **Vamadevan AS, Fukata M, Arnold ET, Thomas LS, Hsu D, Abreu MT.** Regulation of Toll-like receptor 4-associated MD-2 in intestinal epithelial cells: a comprehensive analysis. *Innate Immun* 16: 93–103, 2010. doi:10.1177/1753425909339231.

62. **Wapnir RA, Teichberg S.** Regulation mechanisms of intestinal secretion: implications in nutrient absorption. *J Nutr Biochem* 13: 190–199, 2002. doi:10.1016/S0955-2863(02)00181-X.

63. **Weiss N, Zamponi GW.** Control of low-threshold exocytosis by T-type calcium channels. *Biochim Biophys Acta* 1828: 1579–1586, 2013. doi:10.1016/j.bbamem.2012.07.031.

64. **White JP, Cibelli M, Urban L, Nilius B, McGeown JG, Nagy I.** TRPV4: Molecular Conductor of a Diverse Orchestra. *Physiol Rev* 96: 911–973, 2016. doi:10.1152/physrev.00016.2015.

65. **Wong JM, de Souza R, Kendall CW, Emam A, Jenkins DJ.** Colonic health: fermentation and short chain fatty acids. *J Clin Gastroenterol* 40: 235–243, 2006. doi:10.1097/00004836-200603000-00015.

66. **Yang F, Tang E, Guan K, Wang CY.** IKK beta plays an essential role in the phosphorylation of RelA/p65 on serine 536 induced by lipopolysaccharide. *J Immunol* 170: 5630–5635, 2003. doi:10.4049/jimmunol.170.11.5630.

67. **Zevallos VF, Raker V, Tenzer S, Jimenez-Calvente C, Ashfaq-Khan M, Russel N, Pickert G, Schild H, Steinbrink K, Schuppan D.** Nutritional wheat amylase-trypsin inhibitors promote intestinal inflammation via activation of myeloid cells. *Gastroenterology* 152: 1100–1113.e12, 2017. doi:10.1053/j.gastro.2016.12.006.